Ionospheric tilt measurements: climatology and applications for HF Geolocation

Vadym V. Paznukhov[1], David Altadill[2], Estefania Blanch[2], Charles S. Carrano[1], Keith M. Groves[1], Dwight T. Decker[1]

1) Institute for Scientific Research, Boston College, 140 Commonwealth Ave., Boston, MA, 02467, USA
2) Observatori de l'Ebre, CSIC - Universitat Ramon Llull, Spain

This work was funded by the Intelligence Advance Research Projects Activity (IARPA) under contract FA8650-15-C-9105, United States Air Force

IES 2017 Meeting, Alexandria, VA *9–11 May 2017*

Digisonde Tilt measurements

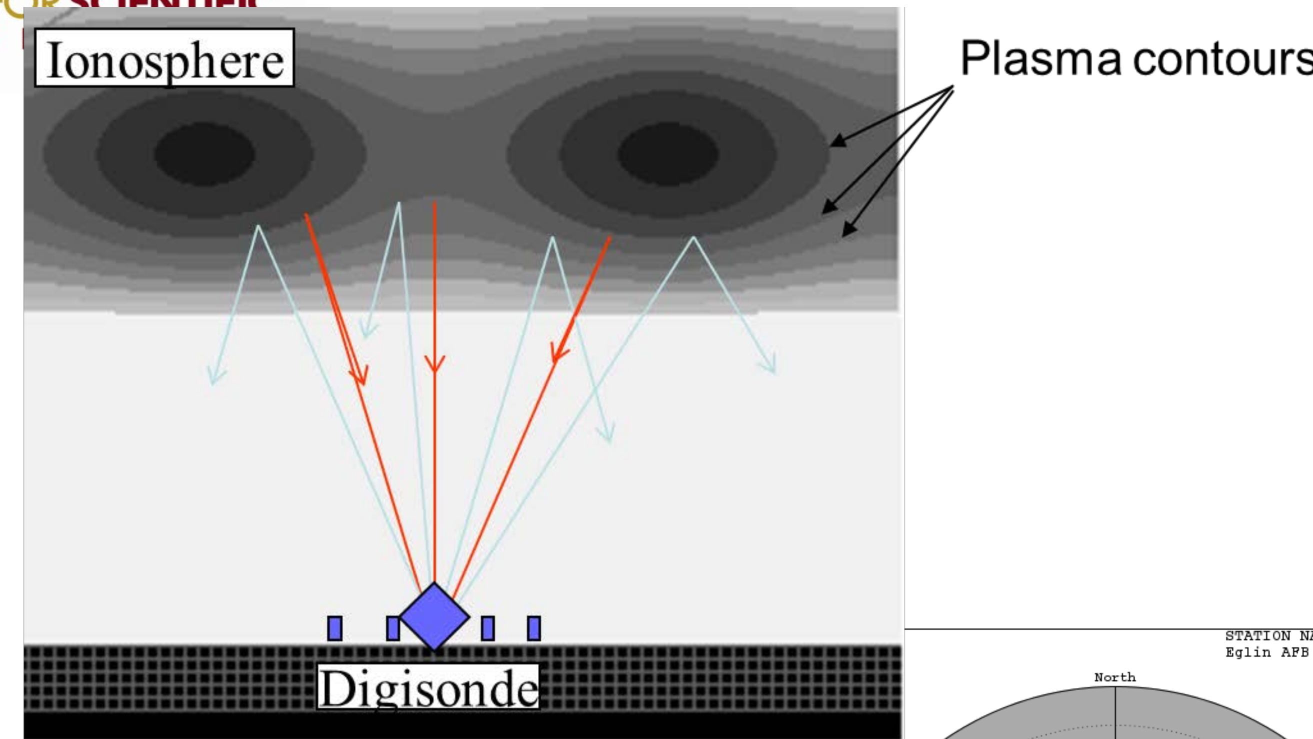

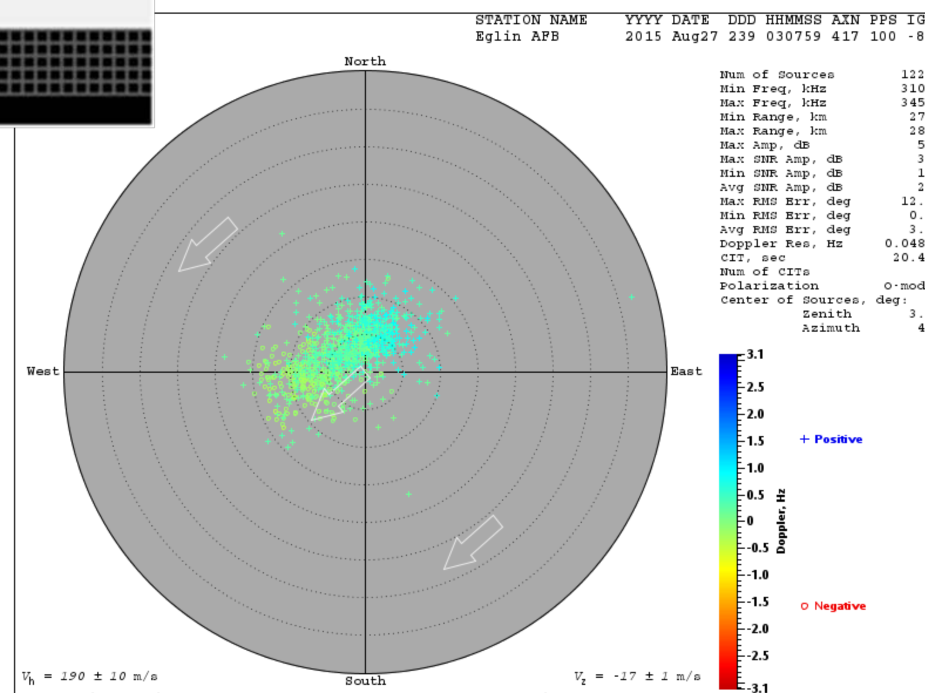

The transmitted signal illuminates a large area in the ionosphere, typically a few hundred kilometers in diameter (top). The transmitted radiowave reflects at every point in the ionosphere where the wave encounters the cut-off frequency (index of reflection is zero). If the normal to the surface of equal electron density points exactly towards the sounder, then the reflected signal can be detected by the system. Each such reflection point is considered as a "source" of a reflected signal. A map showing locations of all "sources" is called a "skymap" (right).

Determining ionospheric tilt from skymap

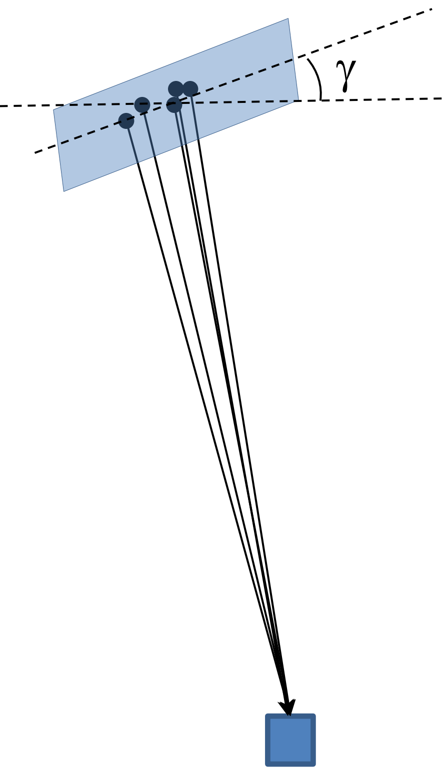

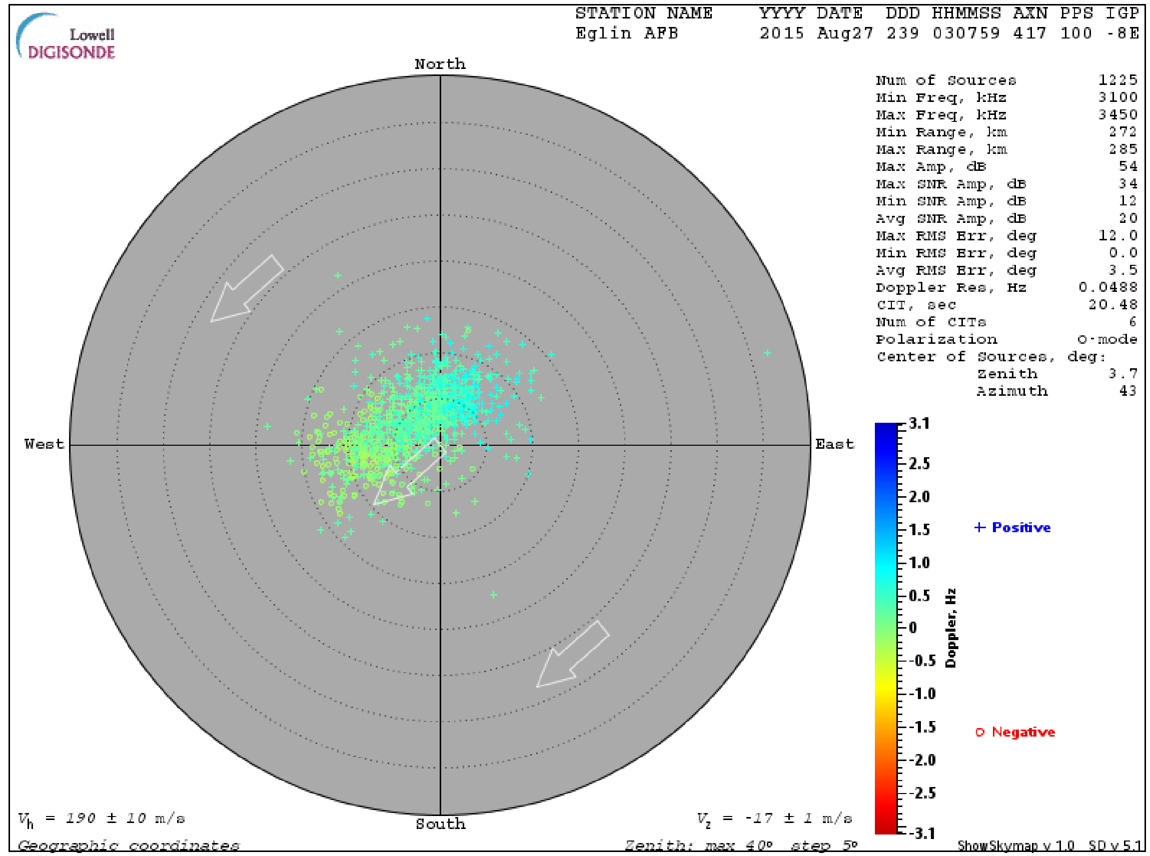

Ionospheric tilt angles specify the orientation of an imaginary surface (left) which reflects radiowaves to produce a specific skymap (right). Tilt angles are found as a center-of-mass" of all the sources present in the skymap data.

Example of strong persistent ionospheric tilt

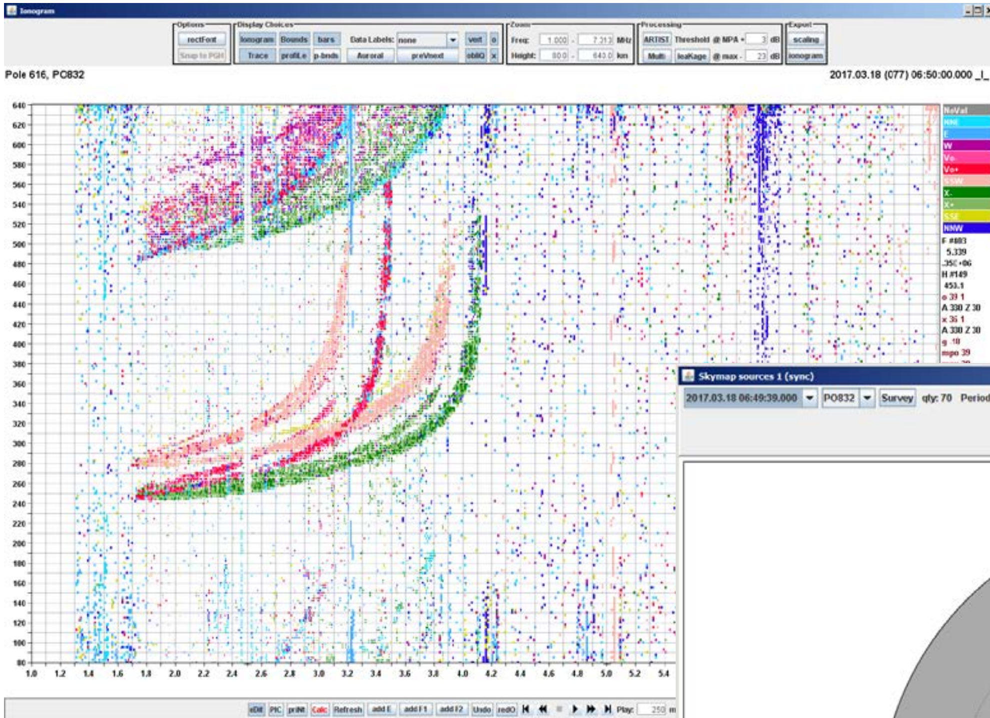

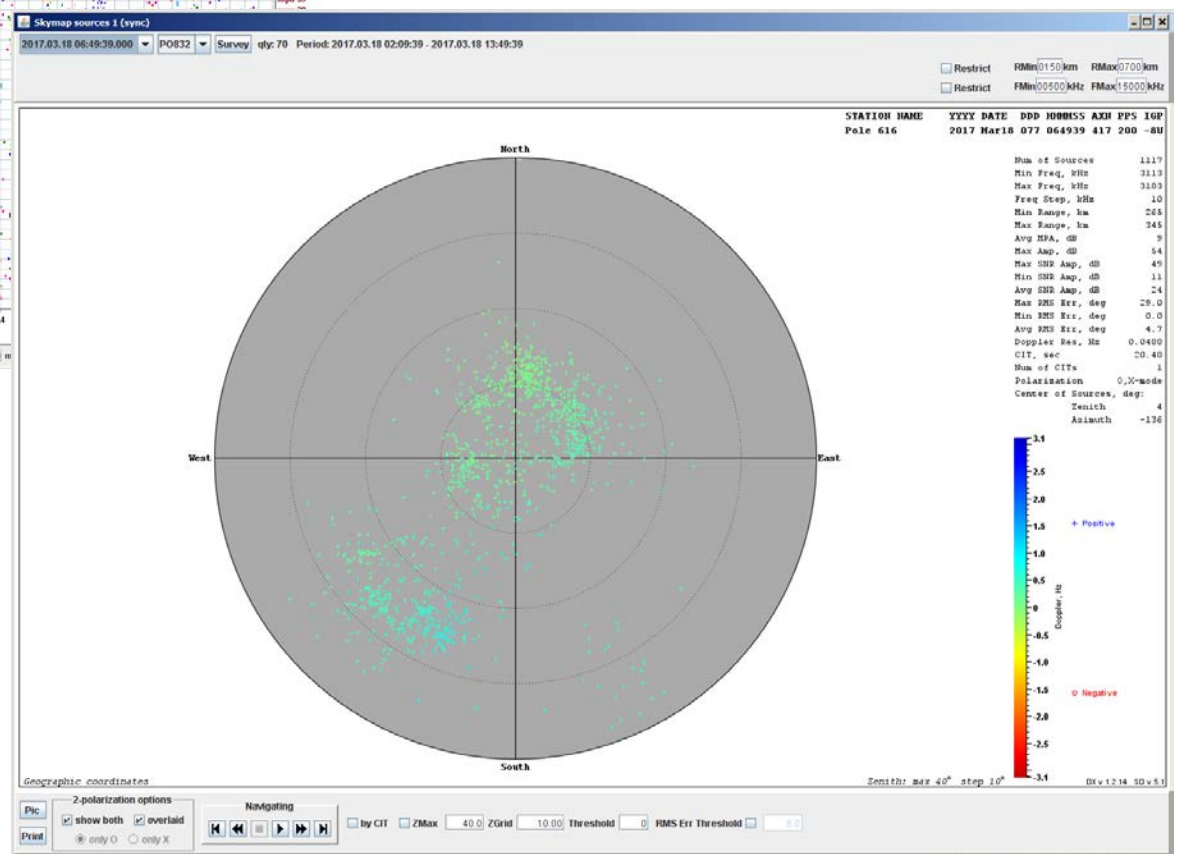

Effect of strong ionospheric tilt

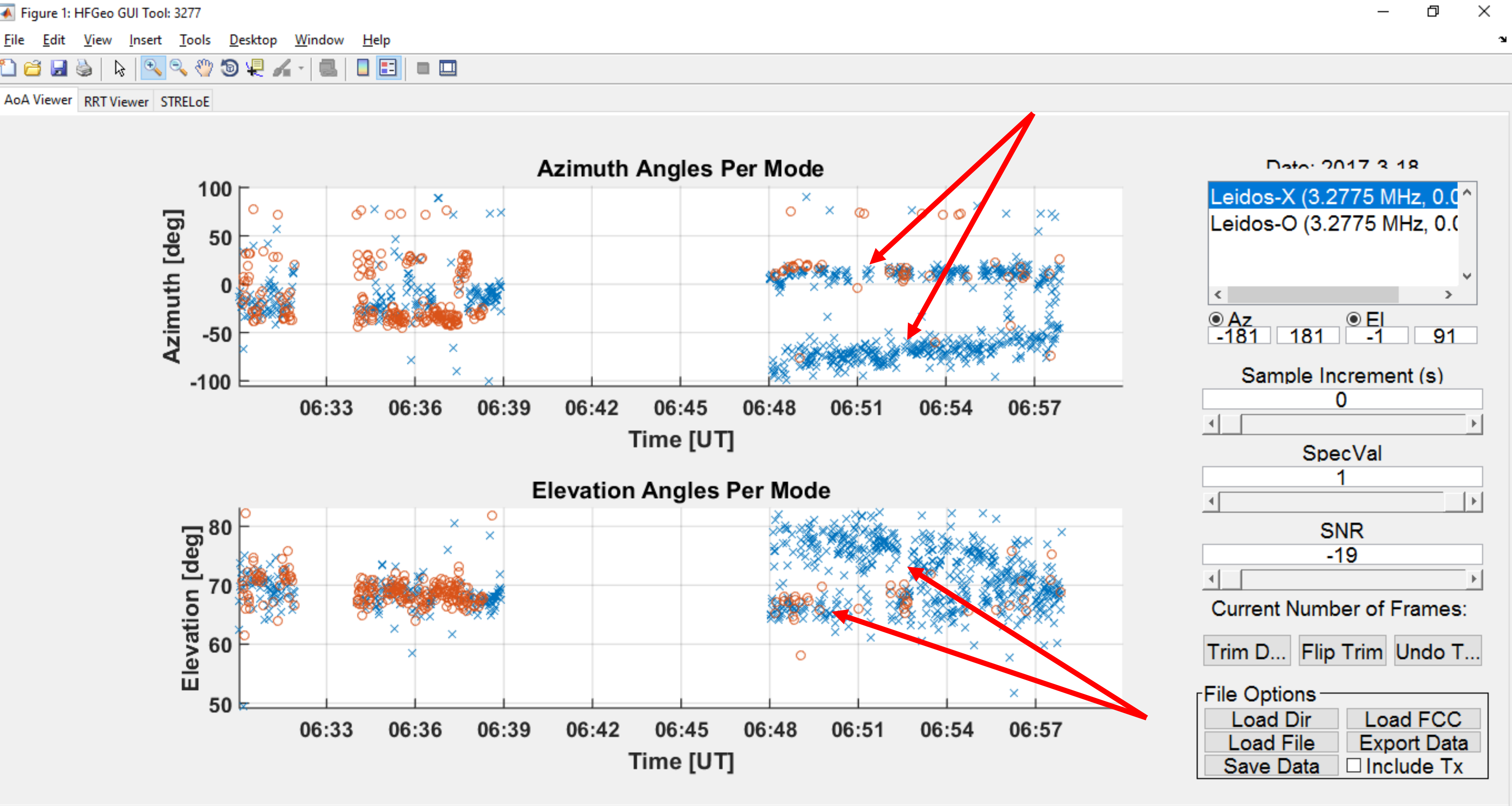

Strong ionospheric tilts result in simultaneous arrival of the signal echoes at two distinct azimuths and zenith angles. Difference in azimuths can be as large as 100 deg.

Importance of ionospheric tilt (horizontal gradients) for raytracing

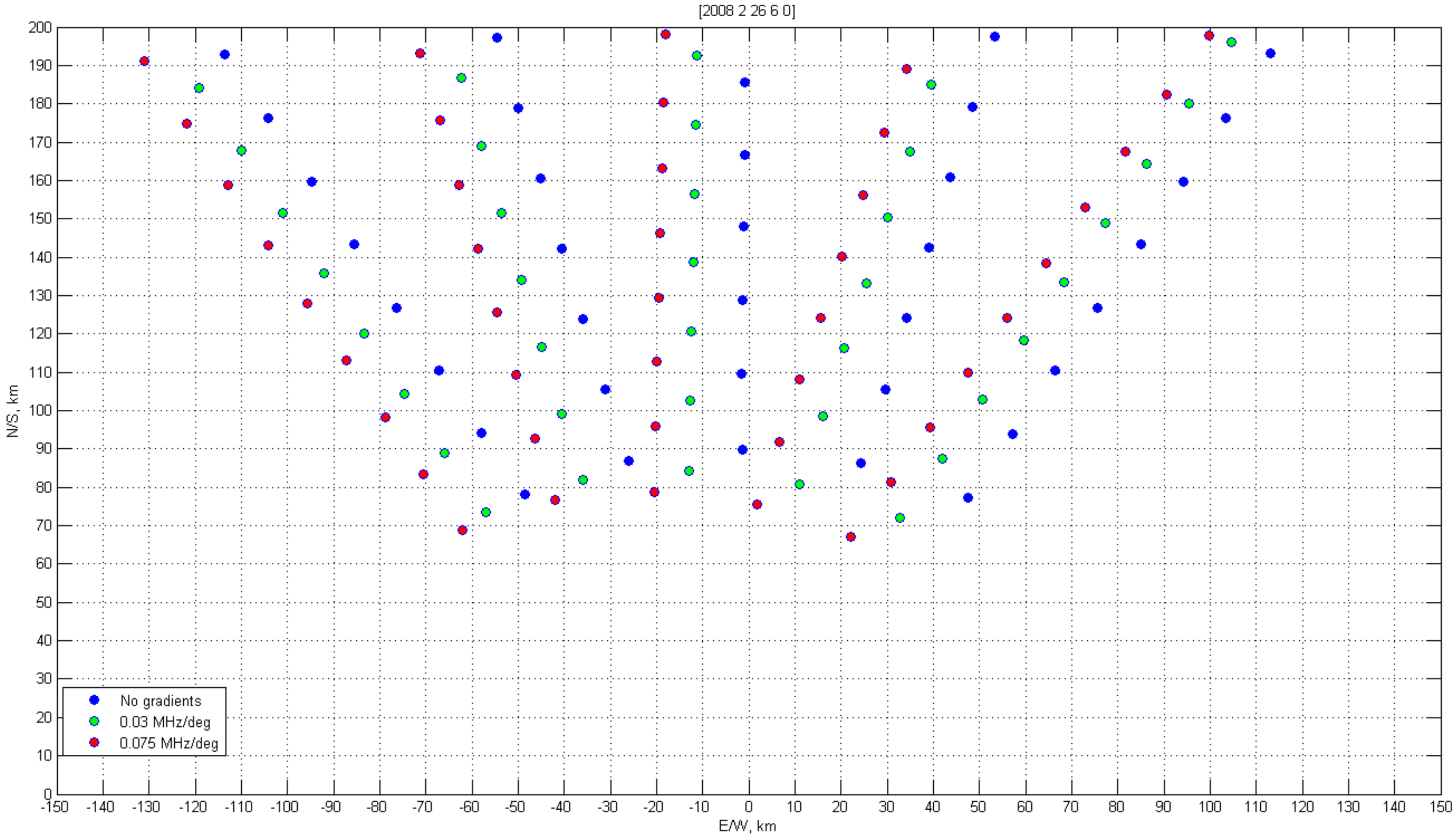

HF rays at 5 MHz operating frequencies are launched for a large range of elevation angles (50-80) and azimuths (-30:30 deg)
For each ray, a landing point is shown in the Cartesian coordinates.
The distance between the landing points generated with no gradients and with the ones present can be as large as 20 km for 0.075MHz/deg gradient and 10 km for 0.03 MHz/deg.

Experiment geometry

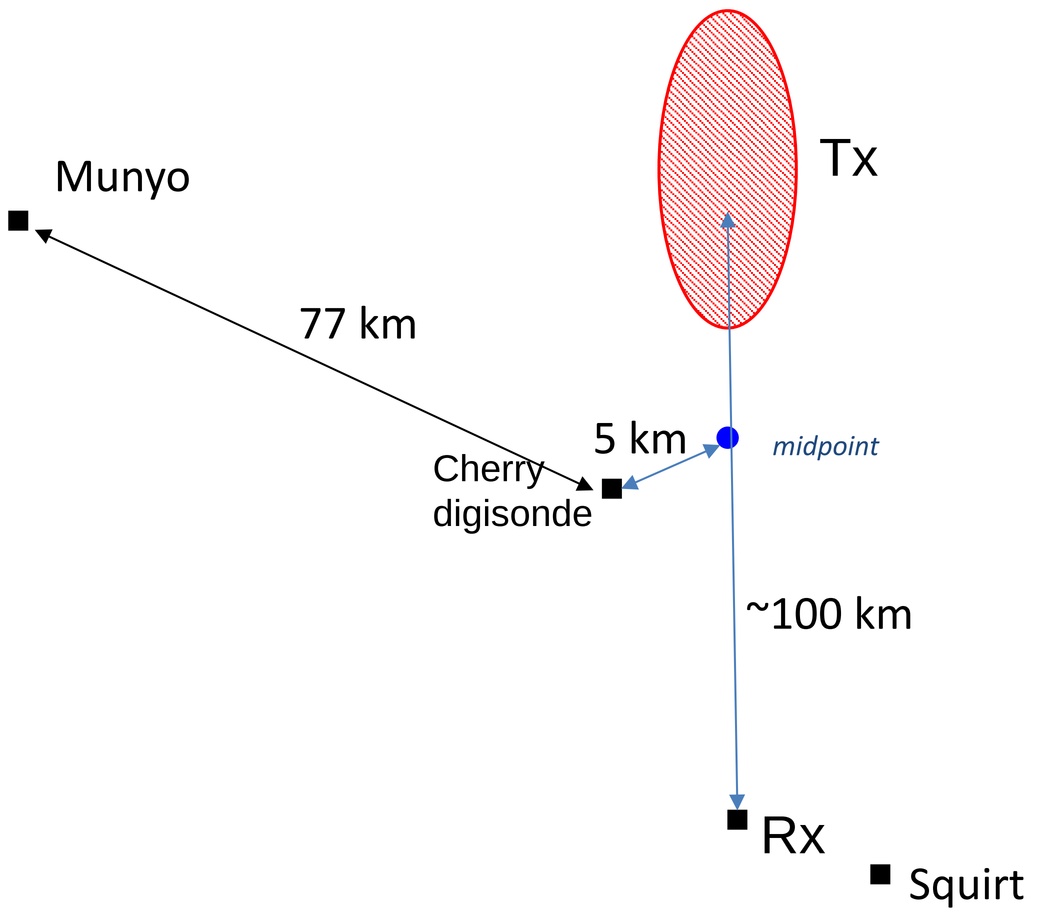

Middle latitudes, 2014

HF AoA observations on January 19, 2014

AoA and Doppler measurements

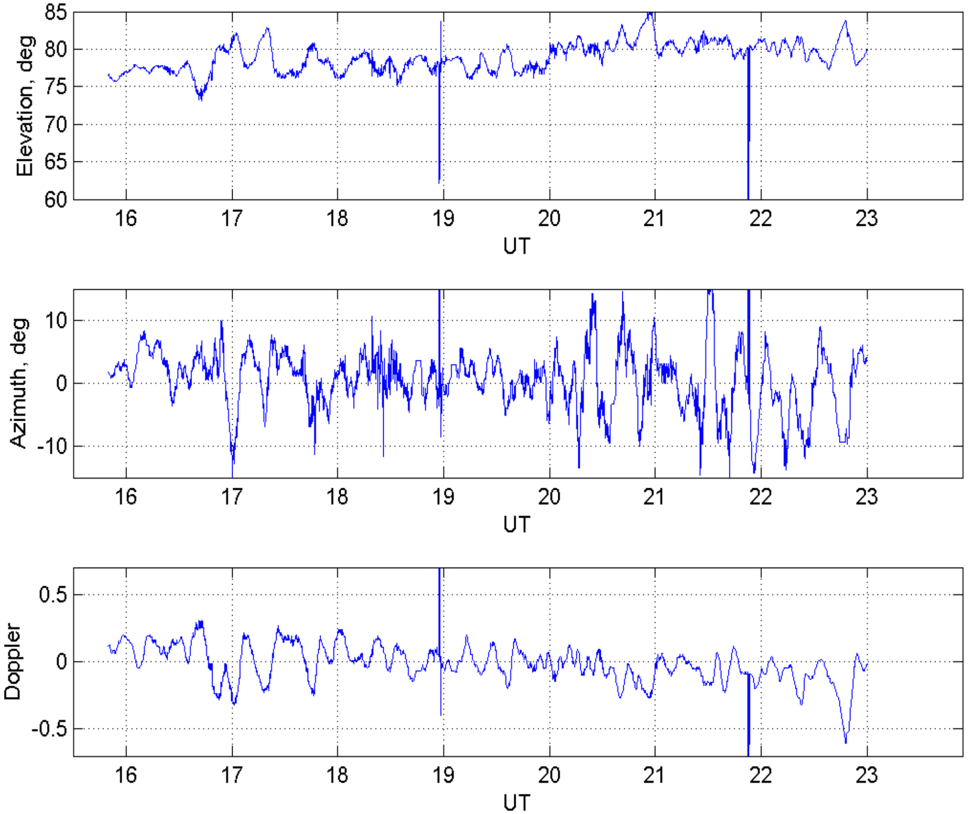

Cherry digisonde observations

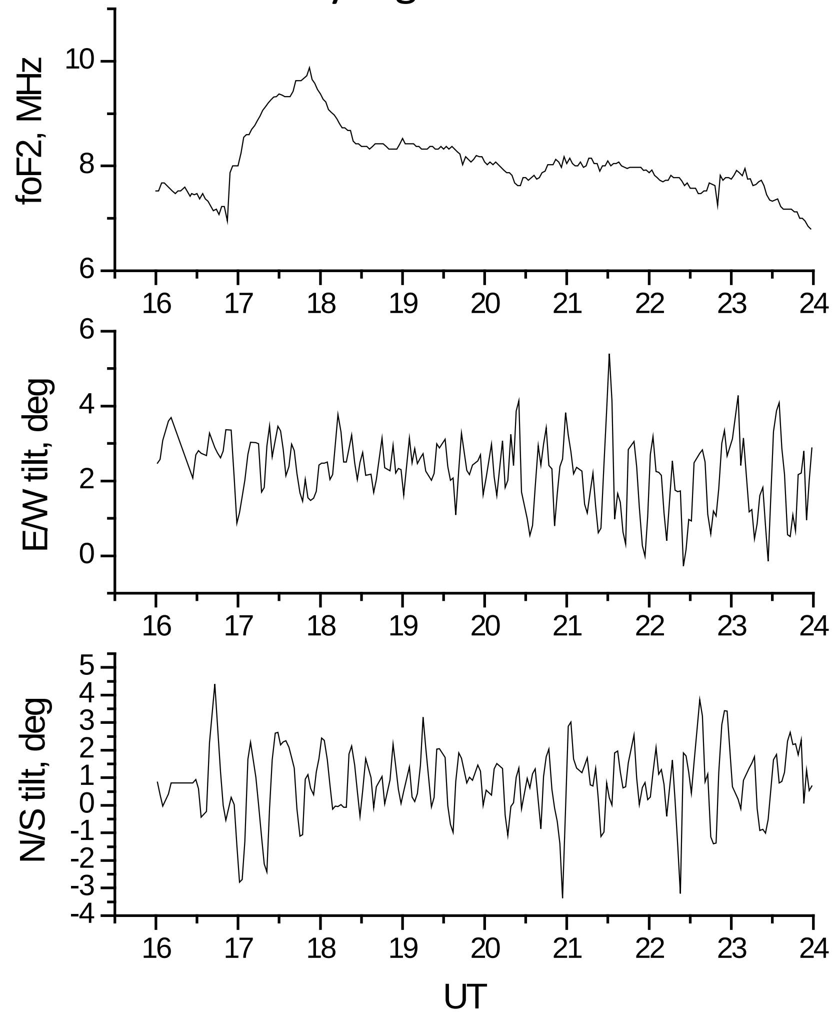

On January 19, 2014, HF link operated at 5.3 MHz (15-20 UT) and at 4.6 MHz (20-23 UT). Moderate TID activity was present during the observation period.

Cherry digisonde was recording standard ionograms (i.e., producing foF2, hmF2, etc) as well as skymap (and tilt) data.

Tilt measurements made on January 26, 2014 at three digisonde locations

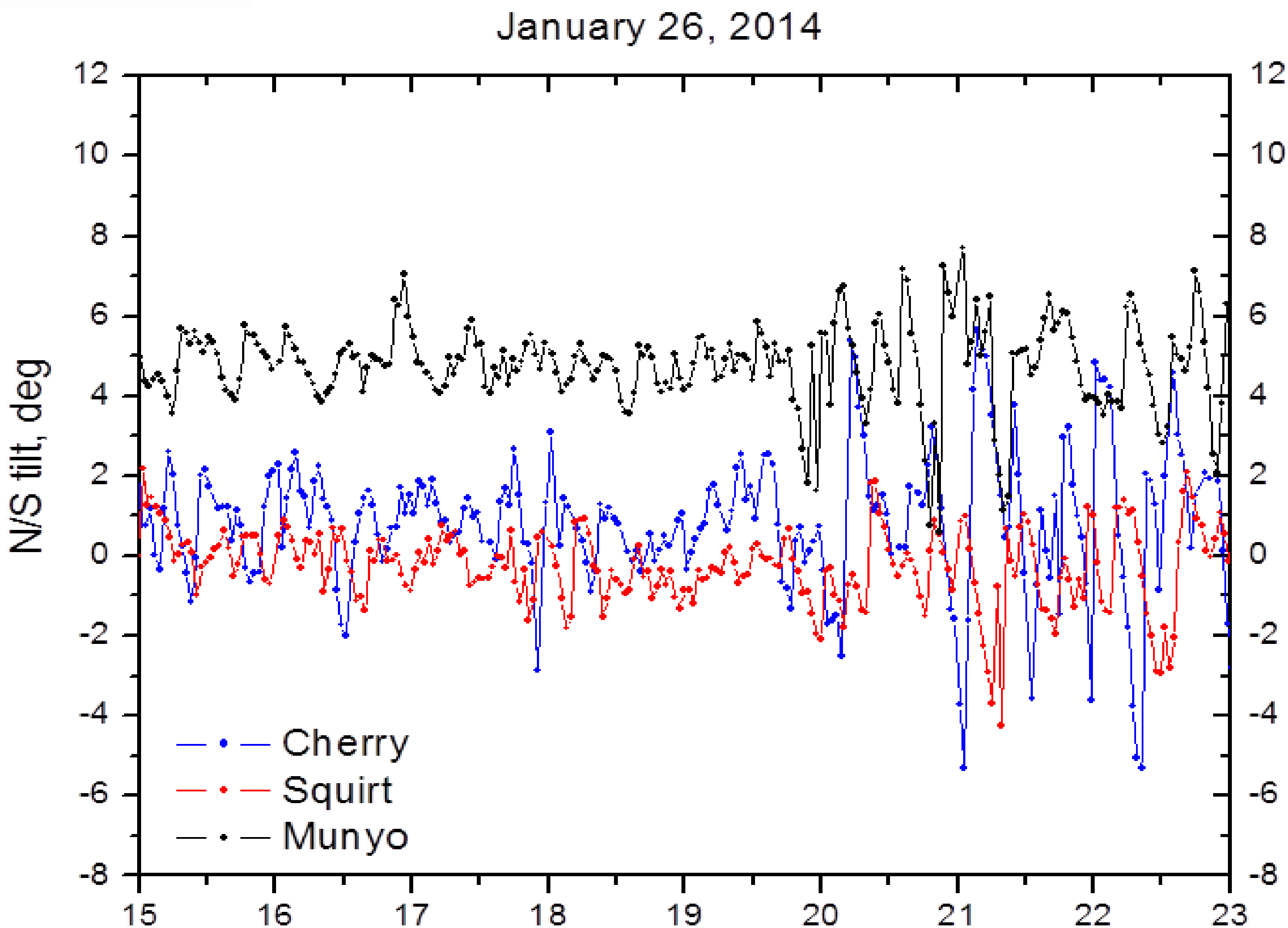

A comparison of tilt measurements at Cherry, Munyo and Squirt sites. Without filtering the noise out, it is difficult to observe the correlation.

Tilt measurements made on January 26, 2014 at two digisonde locations

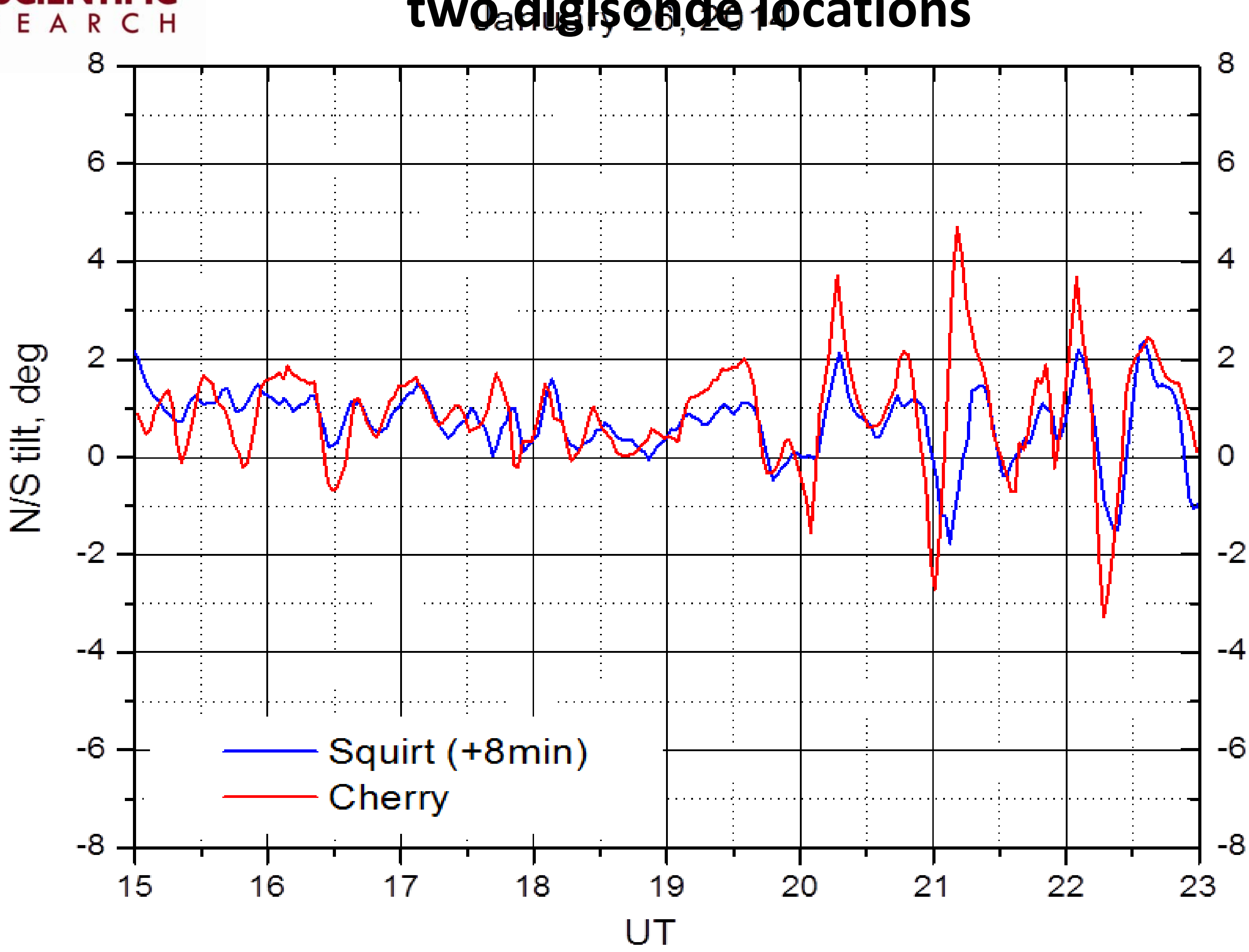

Comparison of tilts measured at Cherry and Squirt location on January 26, 2014. After 19 UT there is a good correlation between two records especially for the stronger variations. NS tilt variations at Squirt lag those at Cherry by approximately 8 minutes indicating North-South propagation of the disturbance.

Tilt measurements are well correlated with AoA data

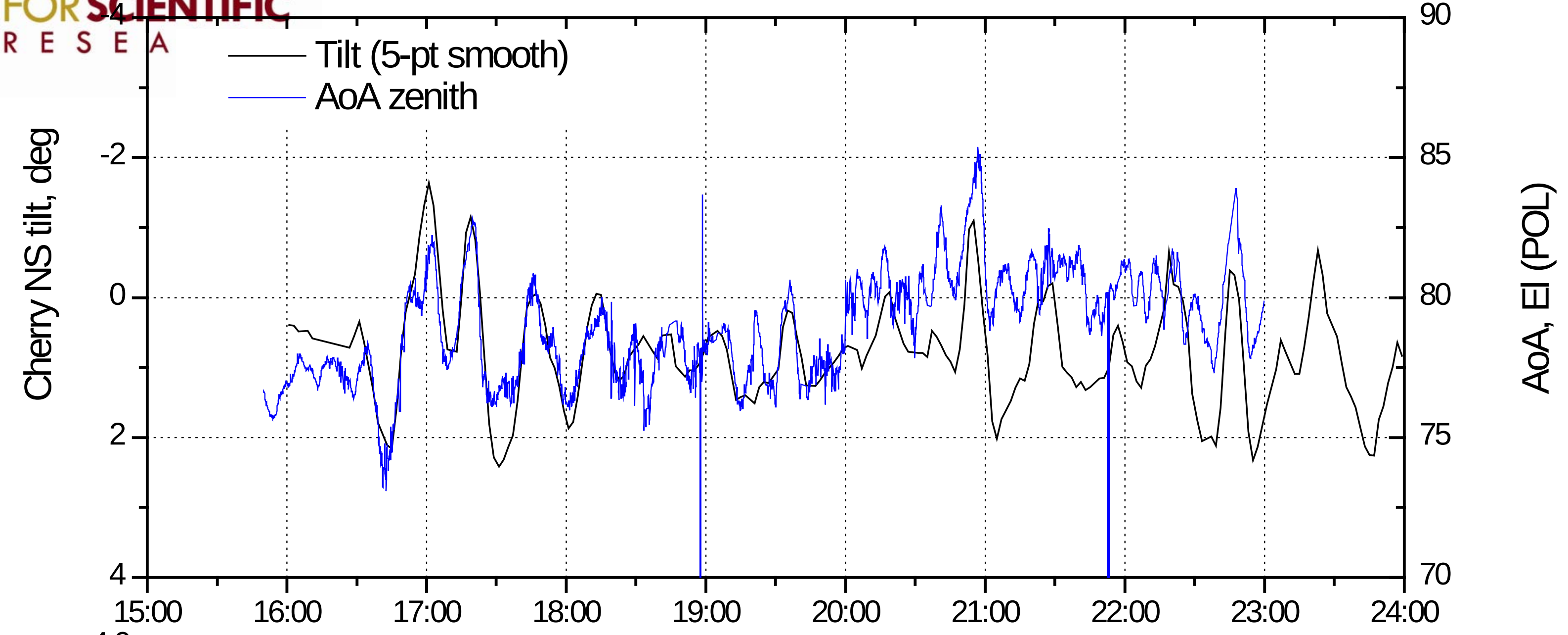

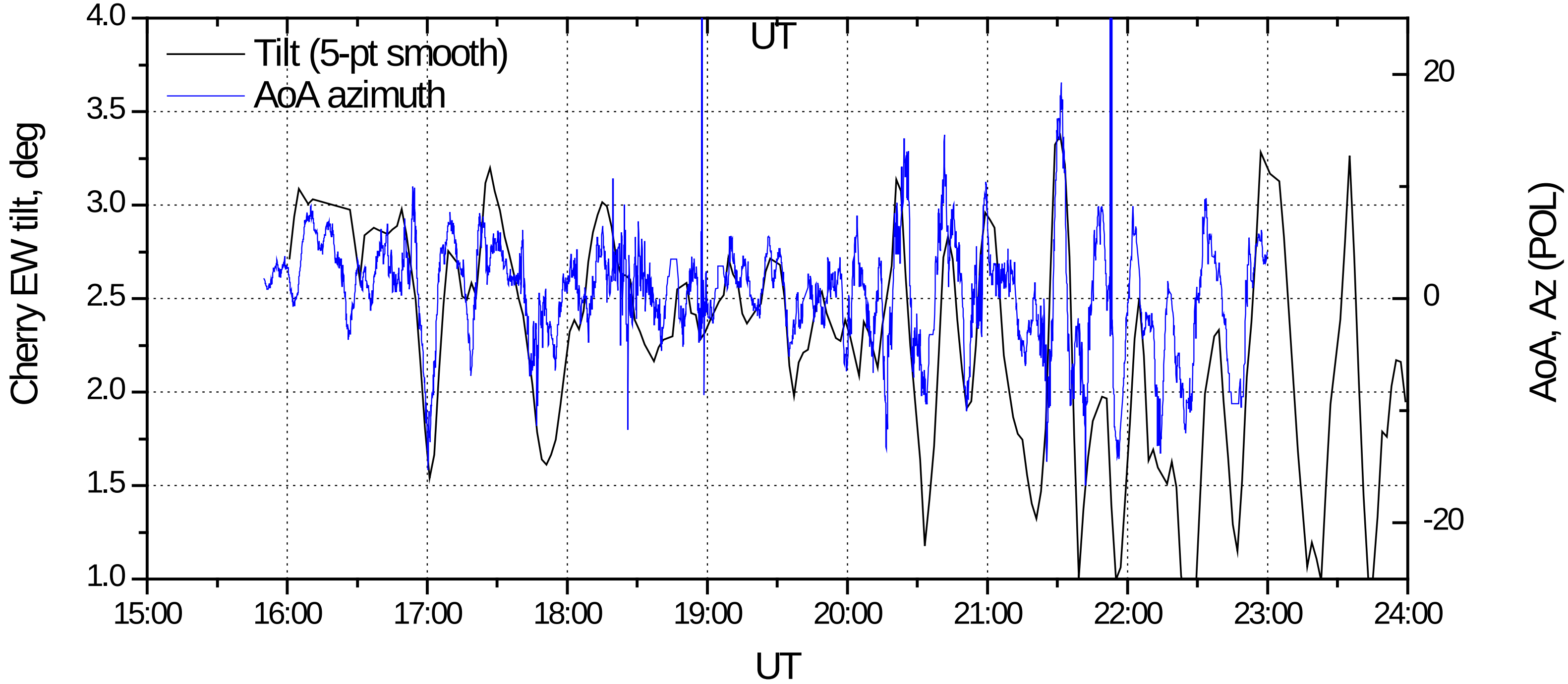

INSTITUTE FOR SCIENTIFIC RESEARCH

Comparison of the measured and reconstructed AoA (El)

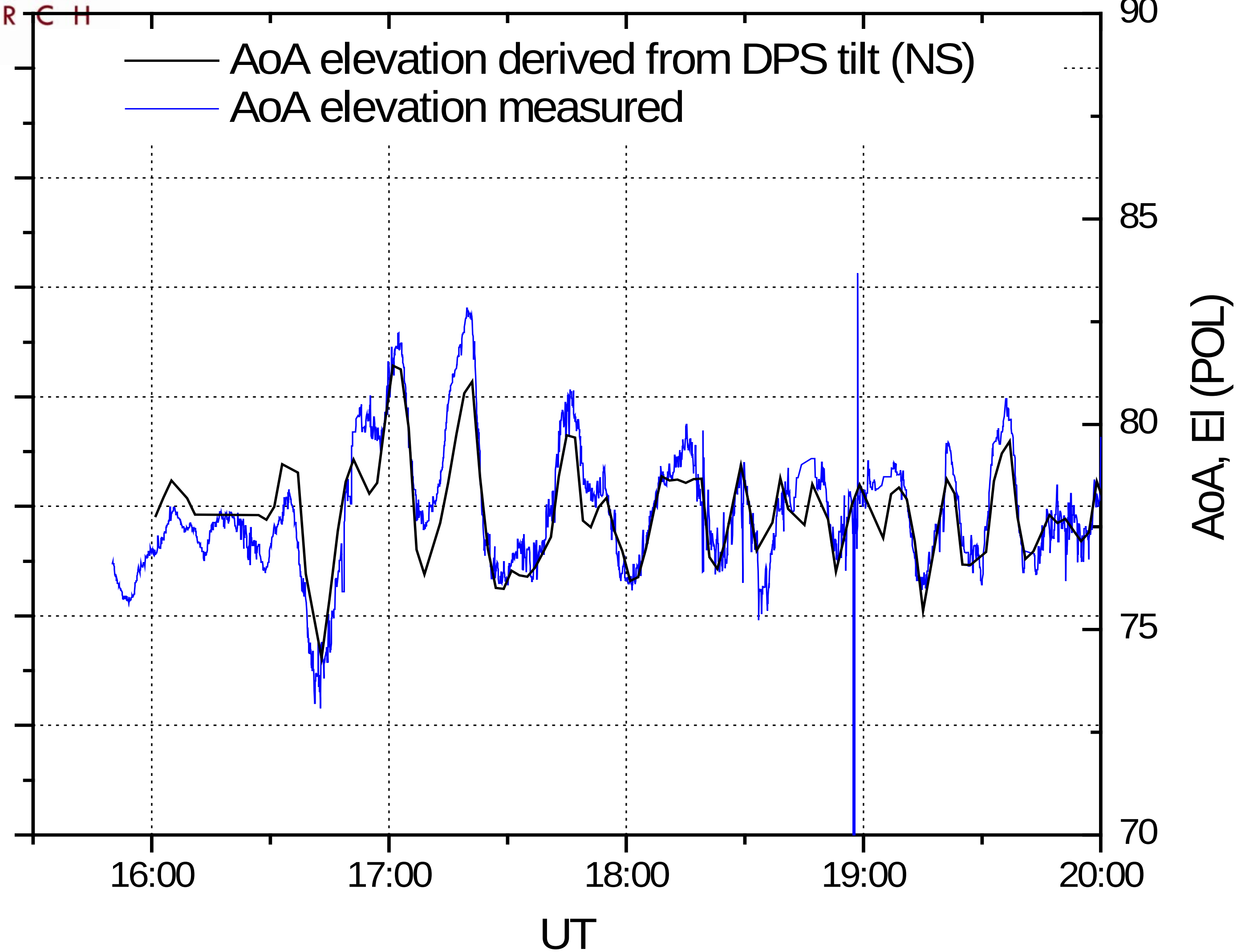

By using fixed Tx and Rx locations and taking tilt variations measured with the digisonde, it is possible to “reconstruct” the expected AoA variations at the Rx location. This example shows the use of the “mirror model” reflection and with the fixed reflection height (250 km). The reflection height can be deduced from ionosonde measurements.

Ionosonde ΔfoF2 data show certain degree of correlation with AoA measurements

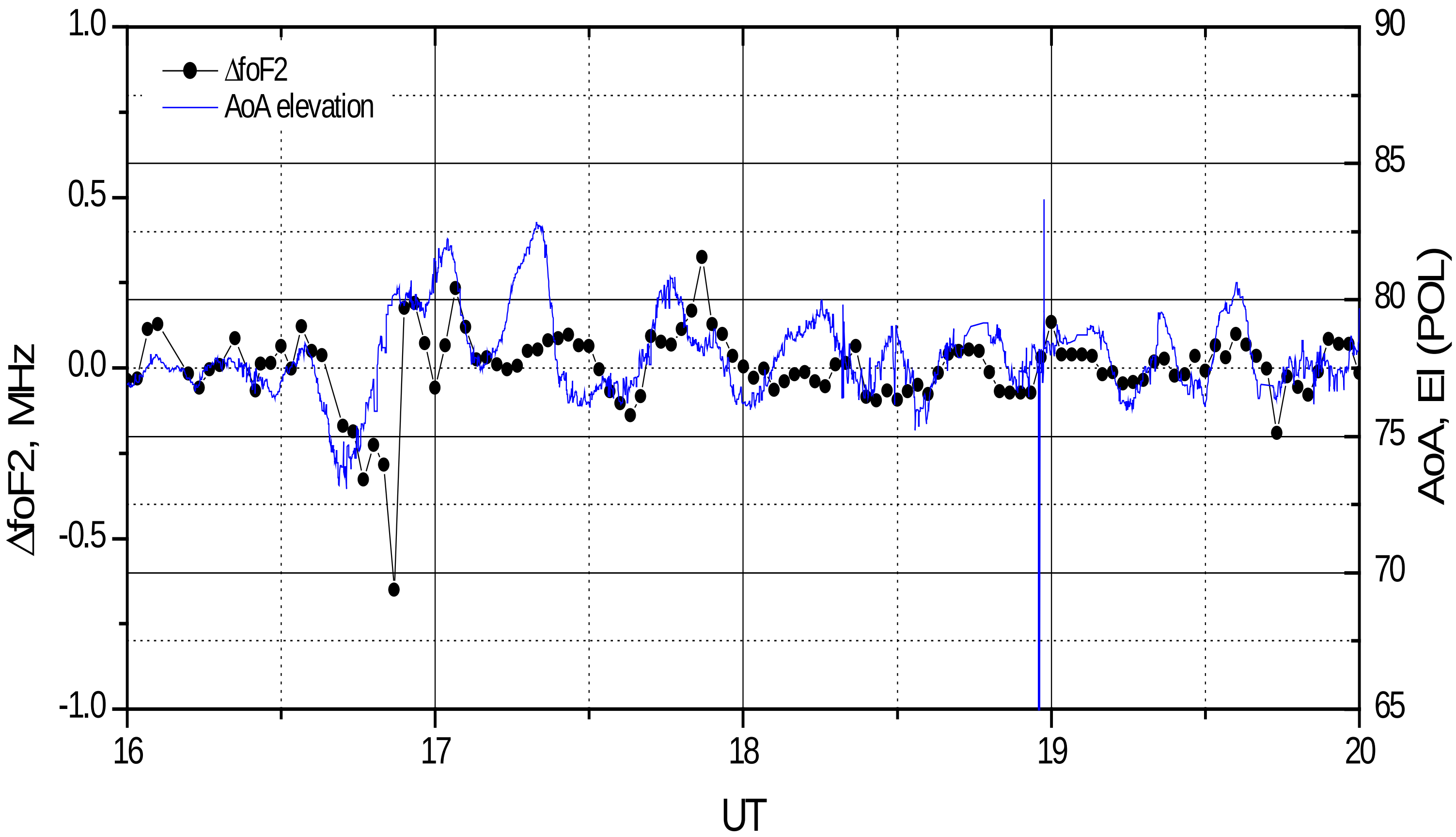

Although the major effect of TIDs is seen in ionospheric height and tilt variations, certain effect is present in the peak density too. This plot illustrates this by comparing relative ΔfoF2 variations (with subtracted daily trend) with AoA (El) observations.

Ebro/Roquetes digisonde station

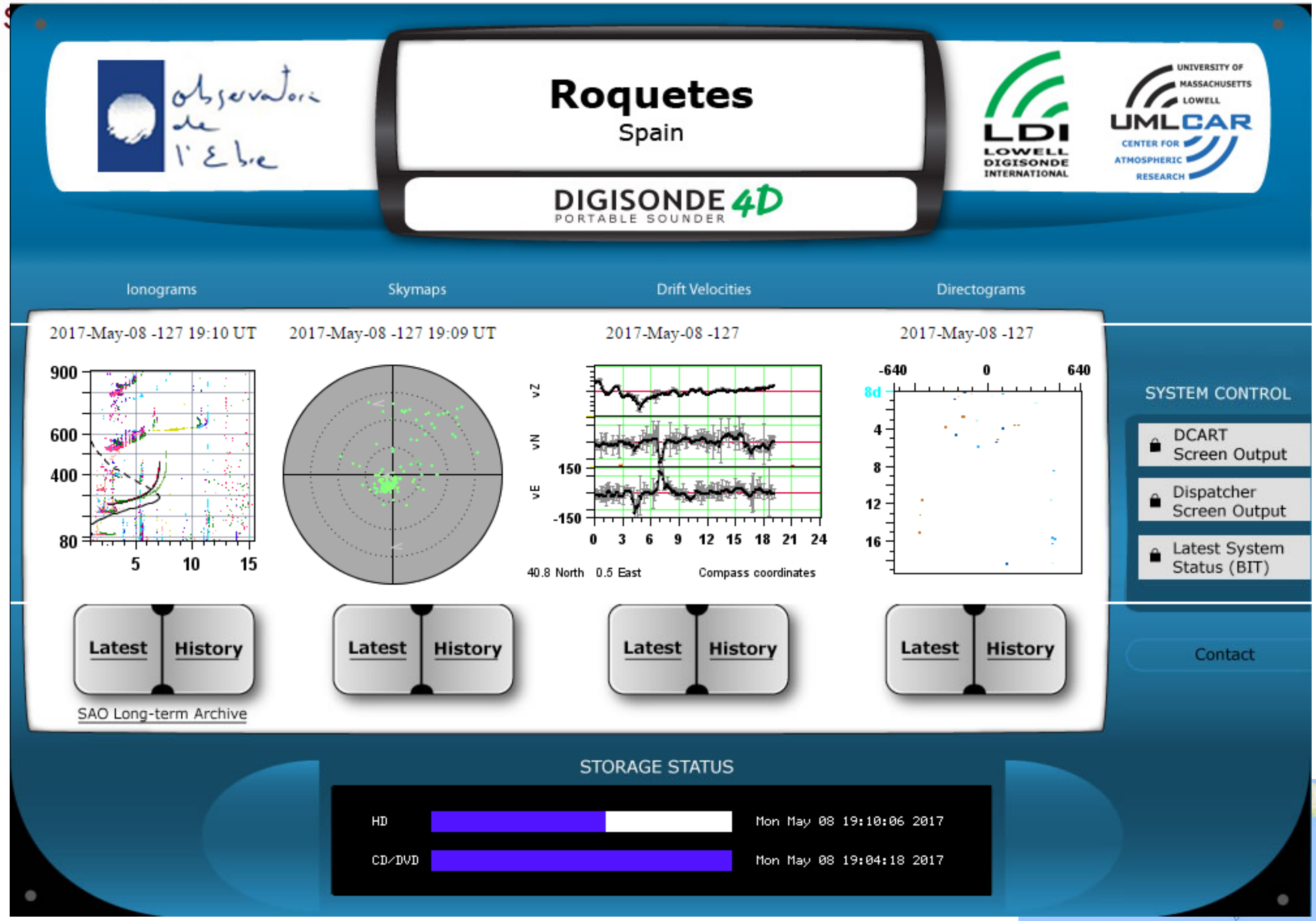

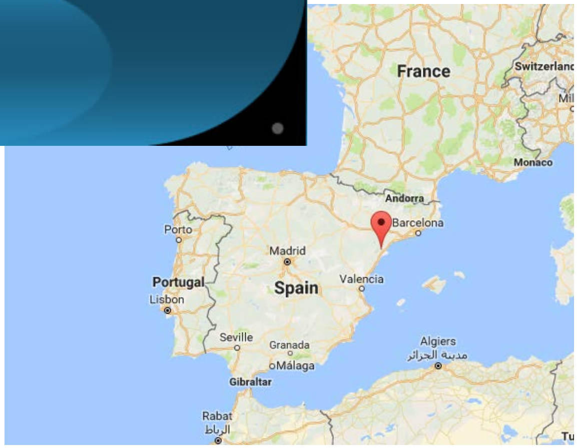

Geographic: latitude = 40.800, longitude = 0.500
Geomagnetic: latitude = 42.885, longitude = 81.696

Ebro station measurements

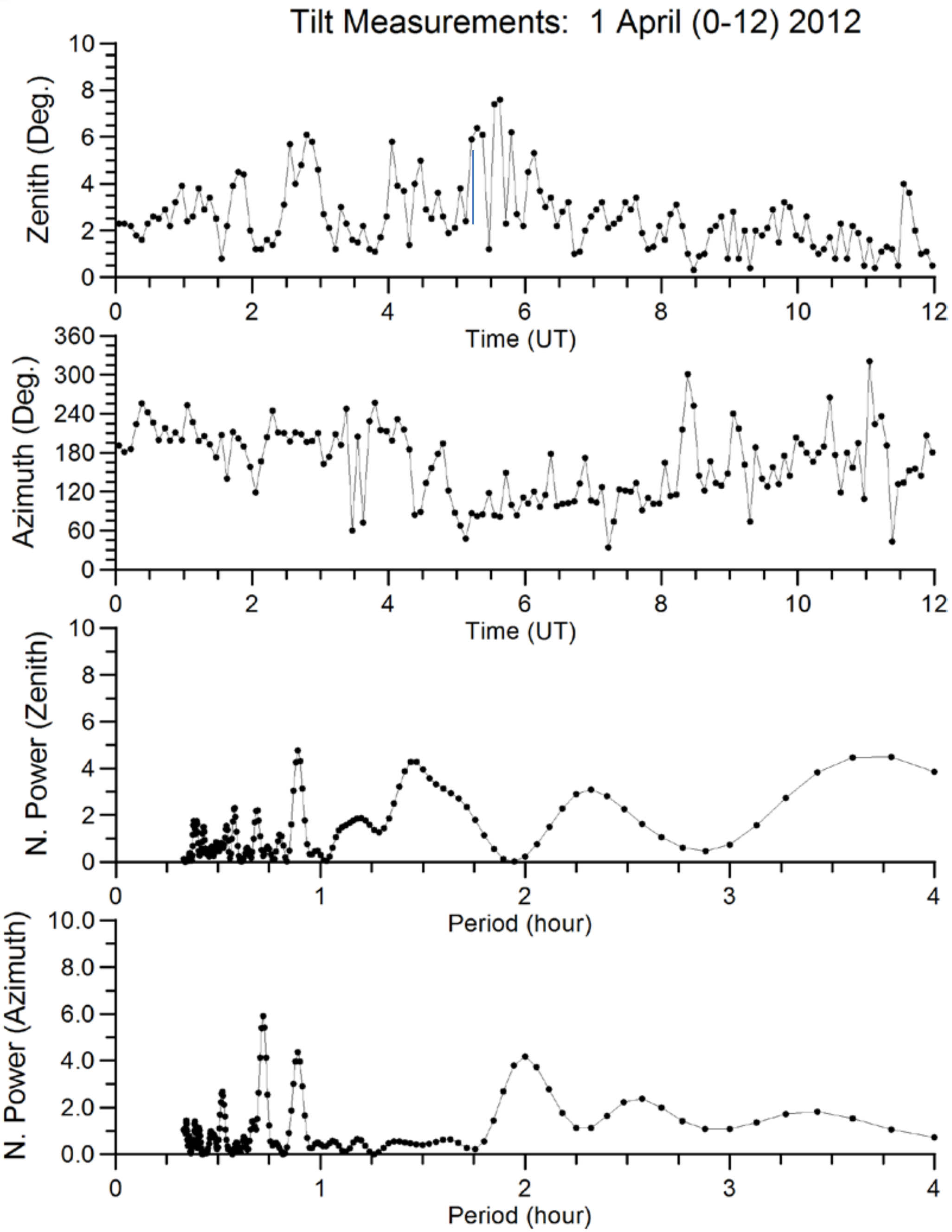

Large tilt variations at sunrise (Ebro station)

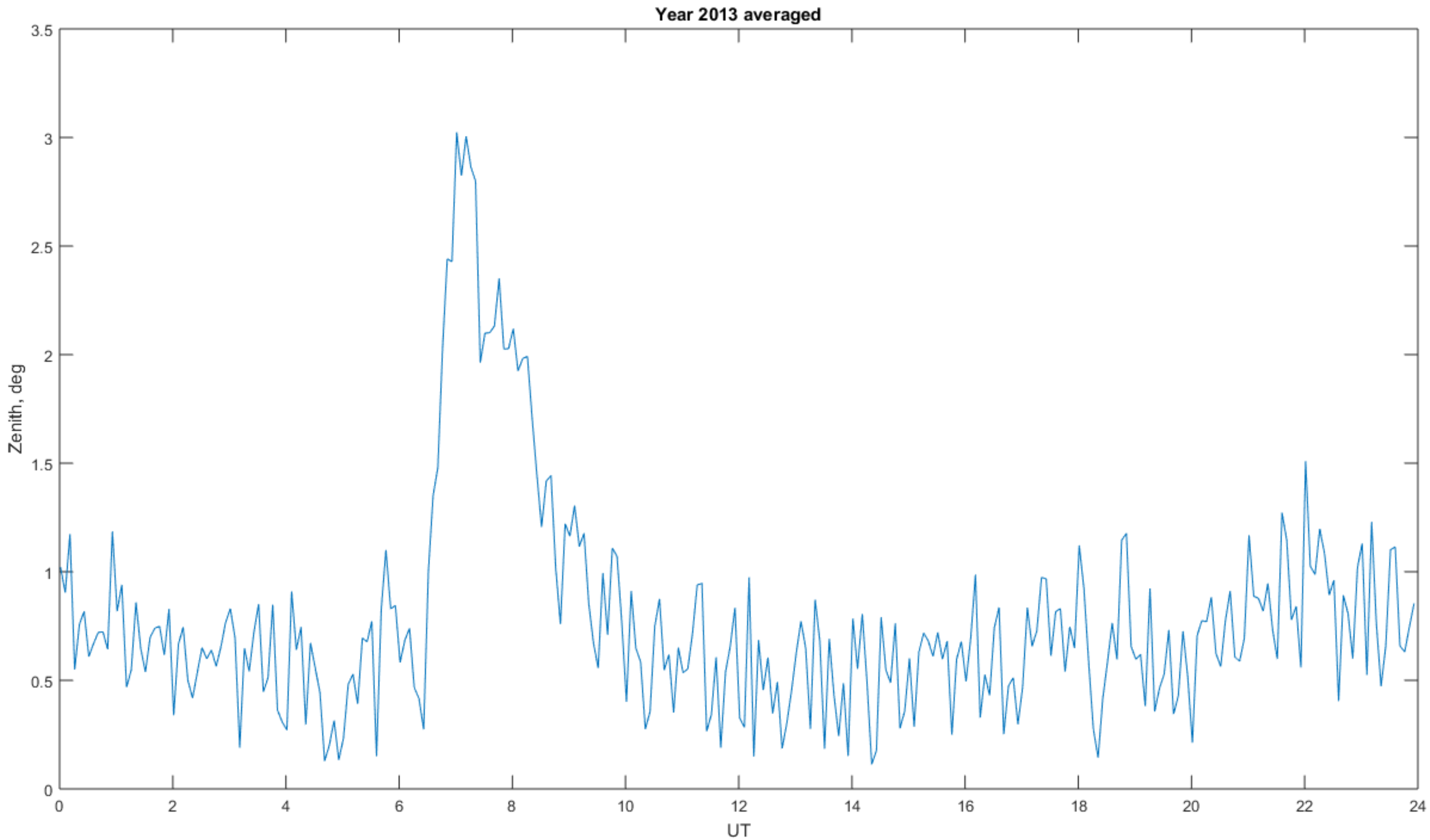

Tilt zenith variations at sunrise can be as large as 3 degree on average

Example of the Ebro tilt spectral analysis

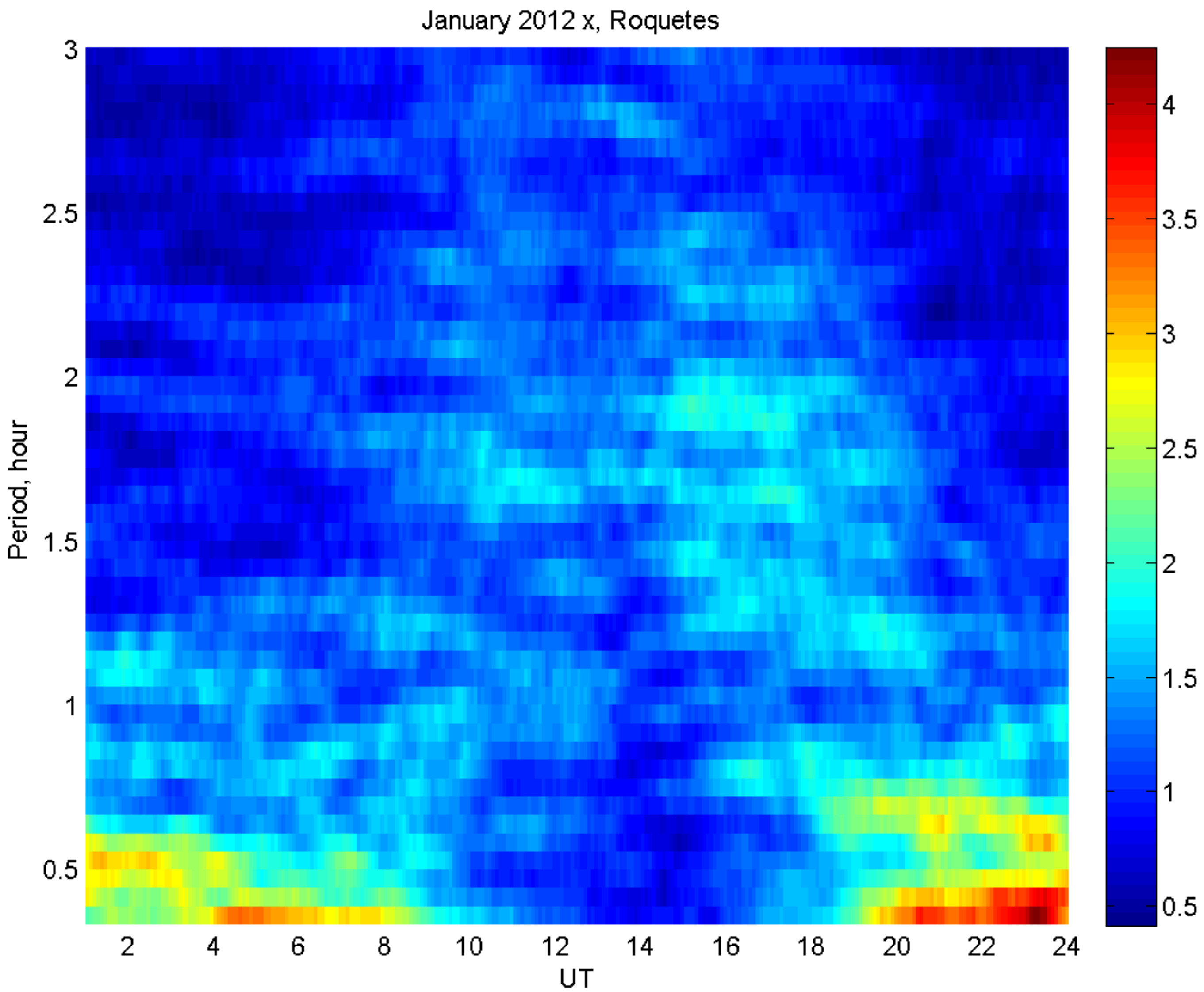

Strong maximum at sunset/ sunrise time (not wave)

Tilt variations at different seasons in 2012

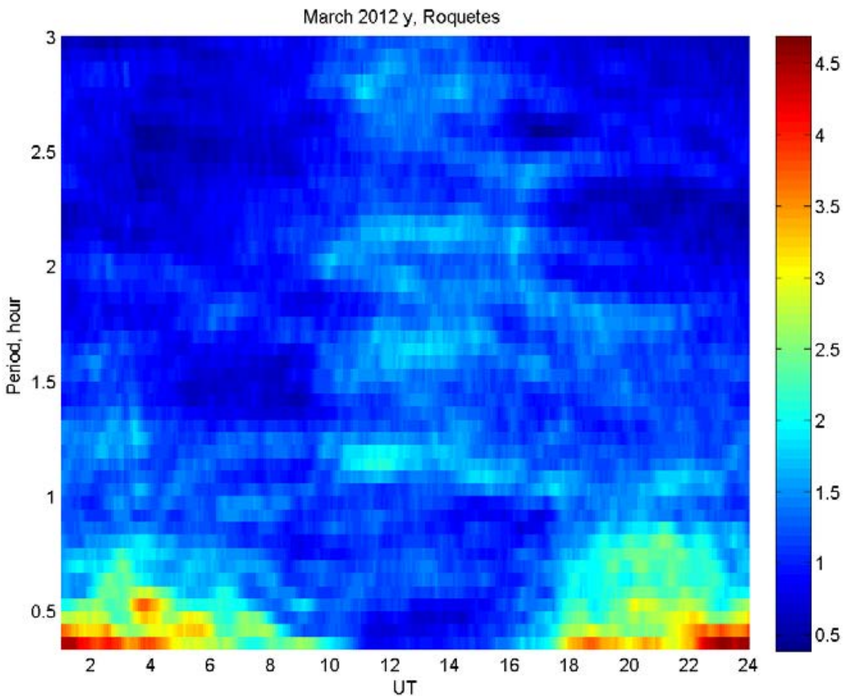

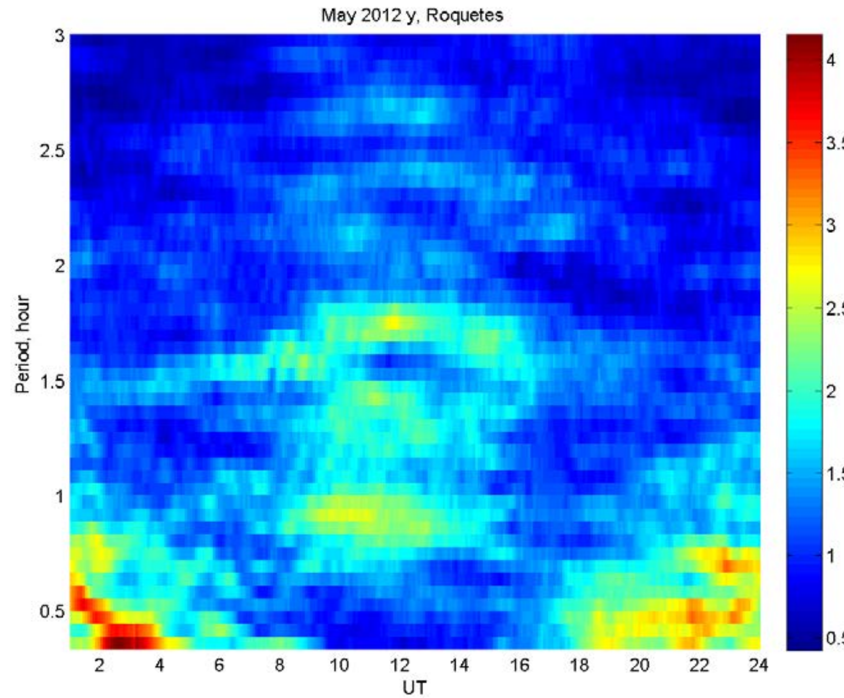

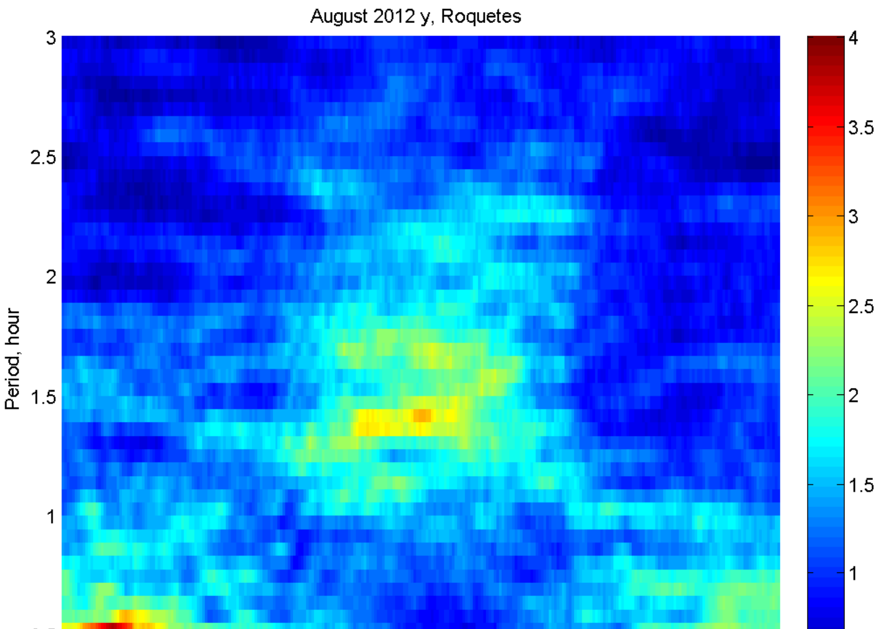

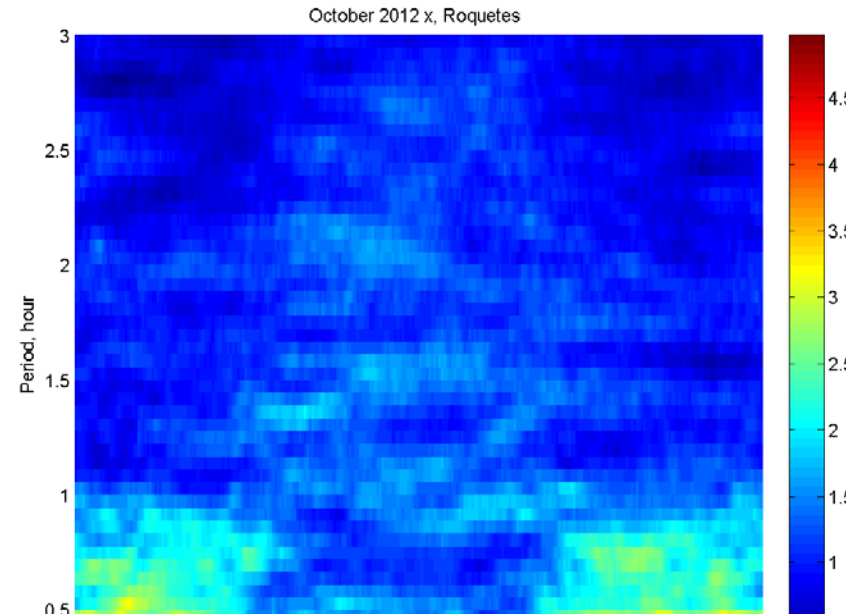

INSTITUTE FOR SCIENTIFIC RESEARCH

Tilt variations for September of 2011-2013

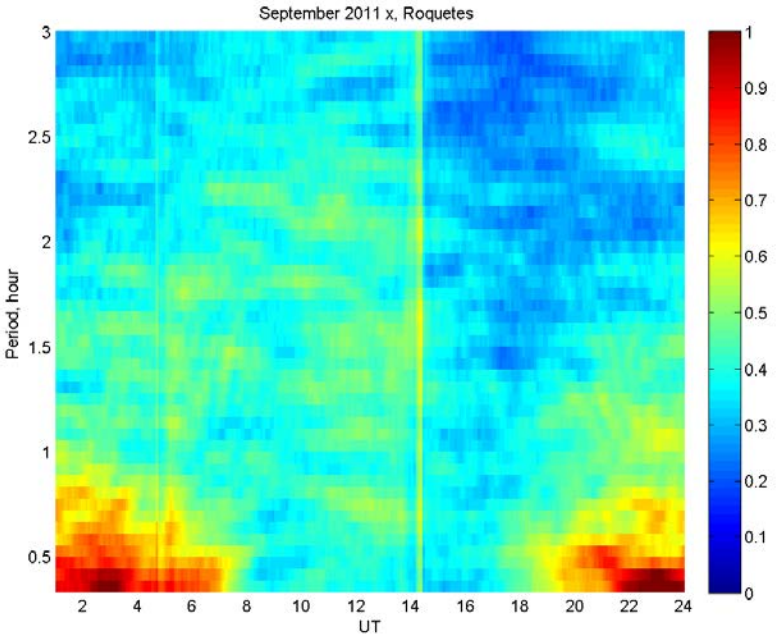

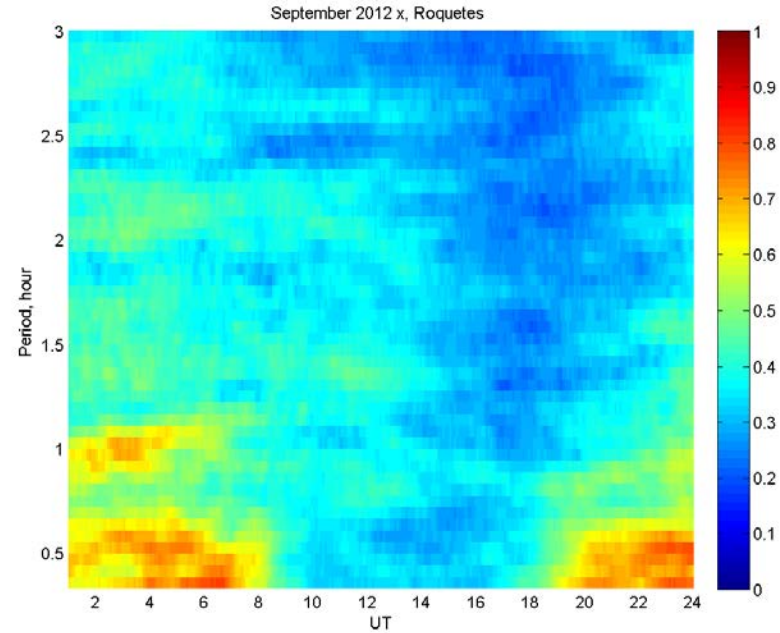

SSN: 120
Ap: 12

SSN: 93.7
Ap: 8

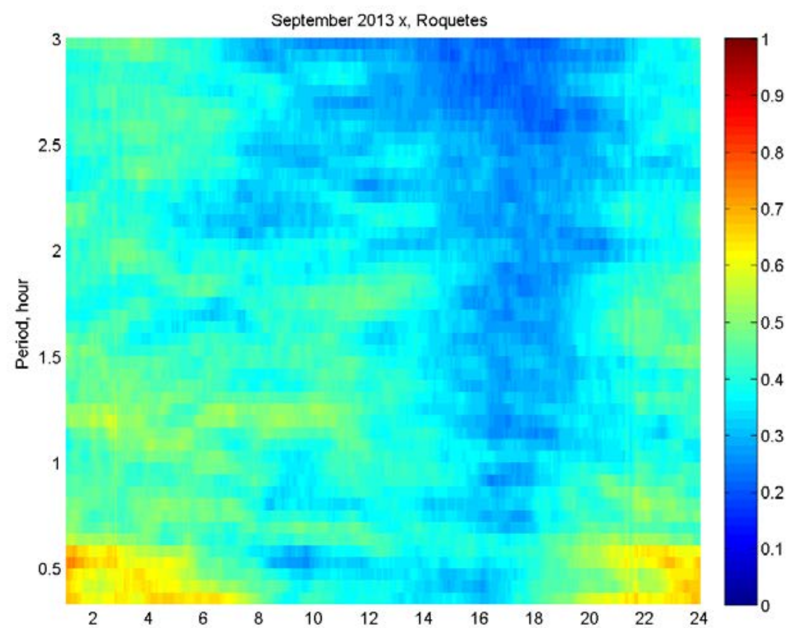

SSN: 54.
Ap: 5

Azimuthal distribution for 2013

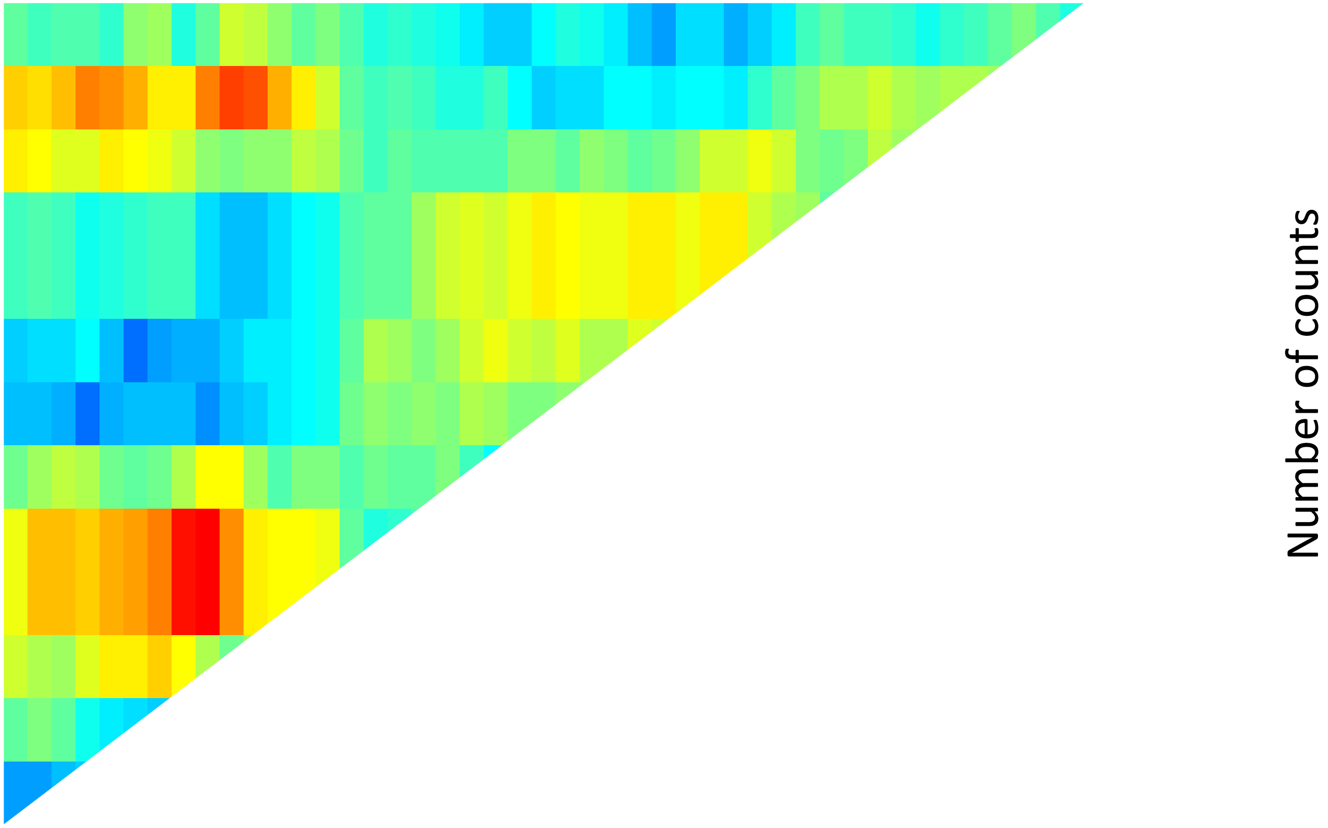

Distribution of the measured tilt azimuths changes through the day.
Possible link to the neutral wind direction?

INSTITUTE FOR SCIENTIFIC RESEARCH

Conclusions

- Digisonde tilt measurements can improve HF geolocation even using simplistic "mirror model" approach. This is illustrated by a comparison of the expected angles of arrival (AoA) to the actual measurements.

- Variations of ionospheric tilts are especially large at sunset. Geolocation during that period is extremely difficult.

- Analysis of the tilt measurements made at Ebro station indicate that most of the disturbances appear after the sunrise and have major periods of 30 min to 1.5 hours.
These characteristics are typical for middle-scale TIDS (MSTIDS).

- Summertime appears to have the most frequent occurrence of the disturbances in the tilts.
Direction of propagation: there is an indications that the disturbances tend to be oriented in the sunward direction, which suggest a possible link to the neutral wind direction.

- Variations in tilt intensity appear to moderately increase with the increase in solar activity and geomagnetic disturbances.

Comparison of North-South (x) and East-West (y) tilt components

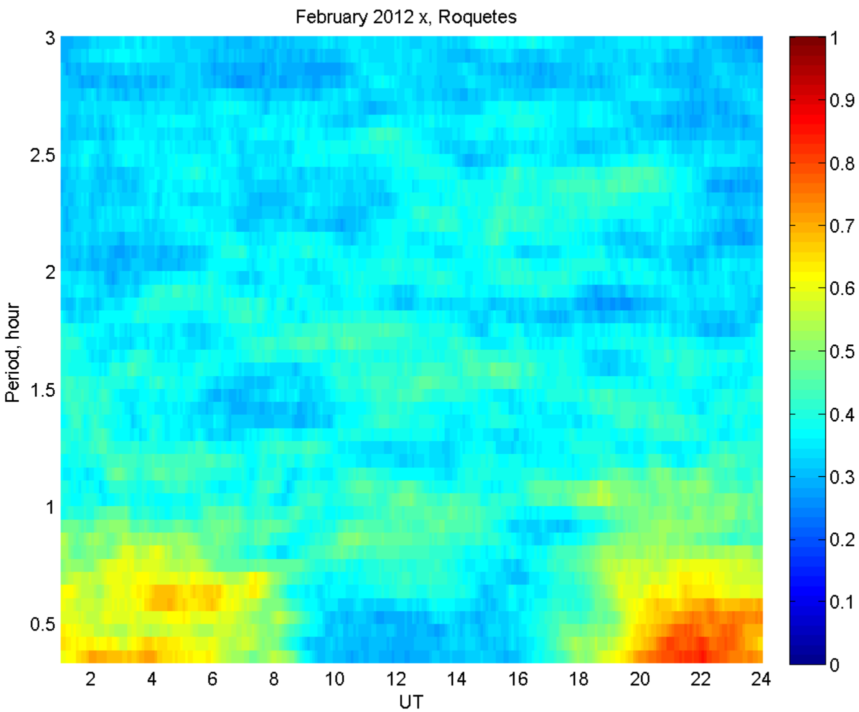

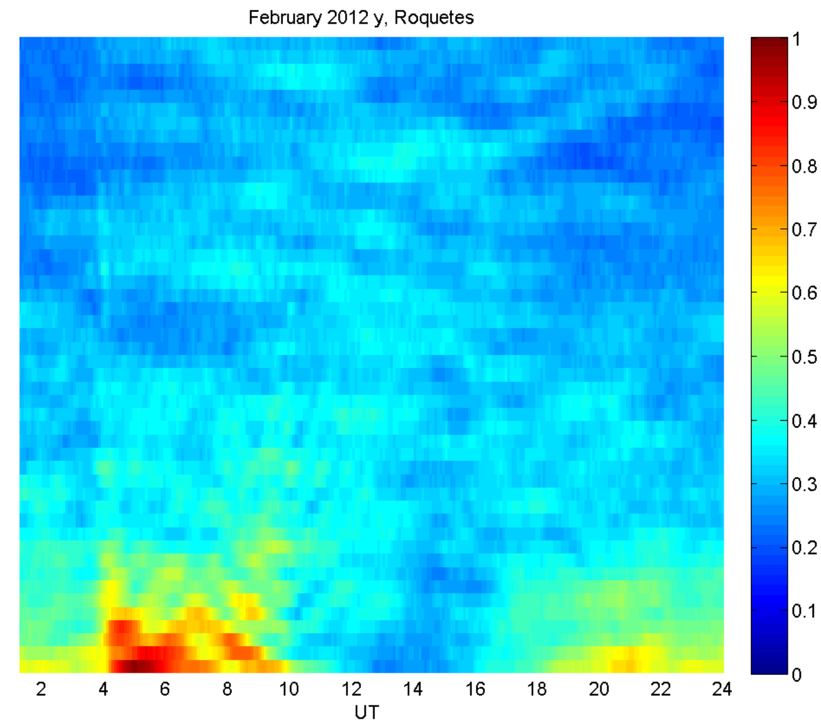

In February, the North-South tilt component demonstrates much stronger disturbances than East-West one, suggesting that in this month, disturbances propagated mostly southward.

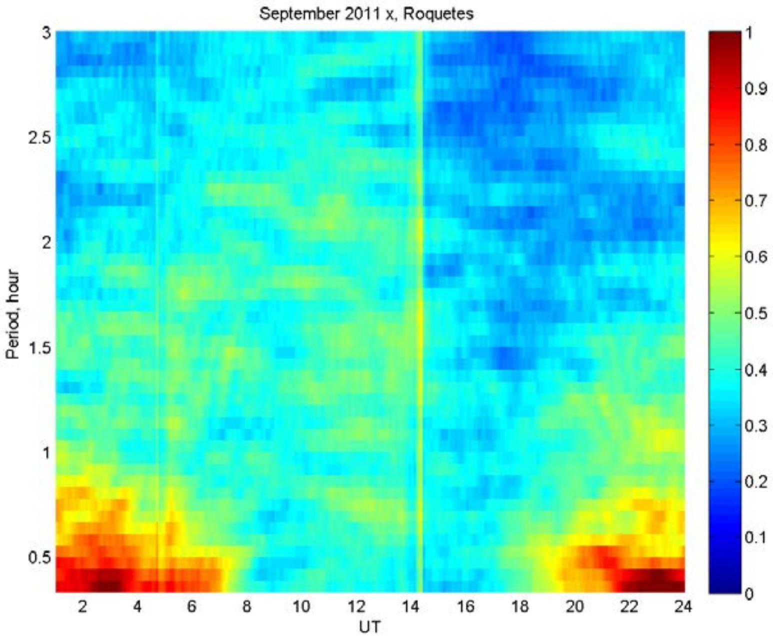
September 2011 x, Roquetes
Period, hour
UT
3
2.5
2
1.5
1
0.5
2 4 6 8 10 12 14 16 18 20 22 24
0 0.1 0.2 0.3 0.4 0.5 0.6 0.7 0.8 0.9 1

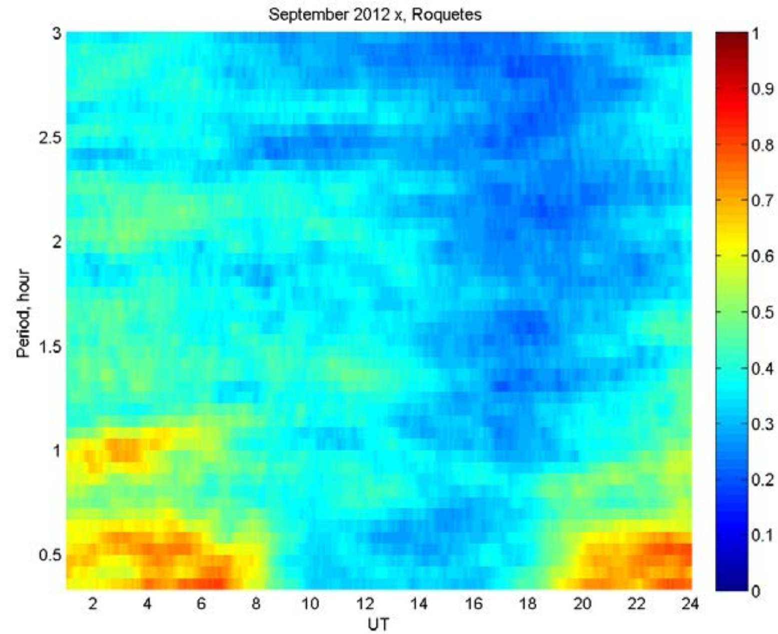
September 2012 x, Roquetes
Period, hour
UT
3
2.5
2
1.5
1
0.5
2 4 6 8 10 12 14 16 18 20 22 24
0 0.1 0.2 0.3 0.4 0.5 0.6 0.7 0.8 0.9 1

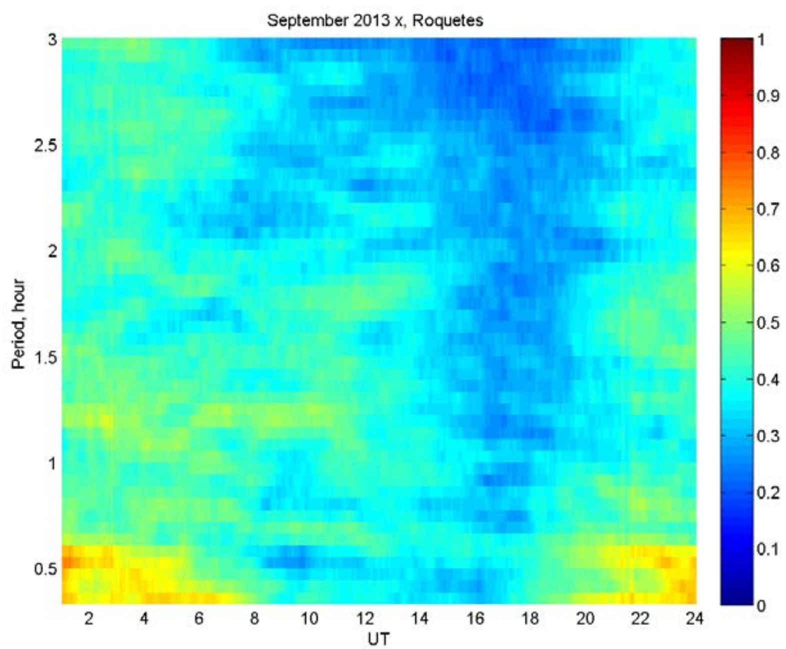
September 2013 x, Roquetes
Period, hour
UT
3
2.5
2
1.5
1
0.5
2 4 6 8 10 12 14 16 18 20 22 24
0 0.1 0.2 0.3 0.4 0.5 0.6 0.7 0.8 0.9 1

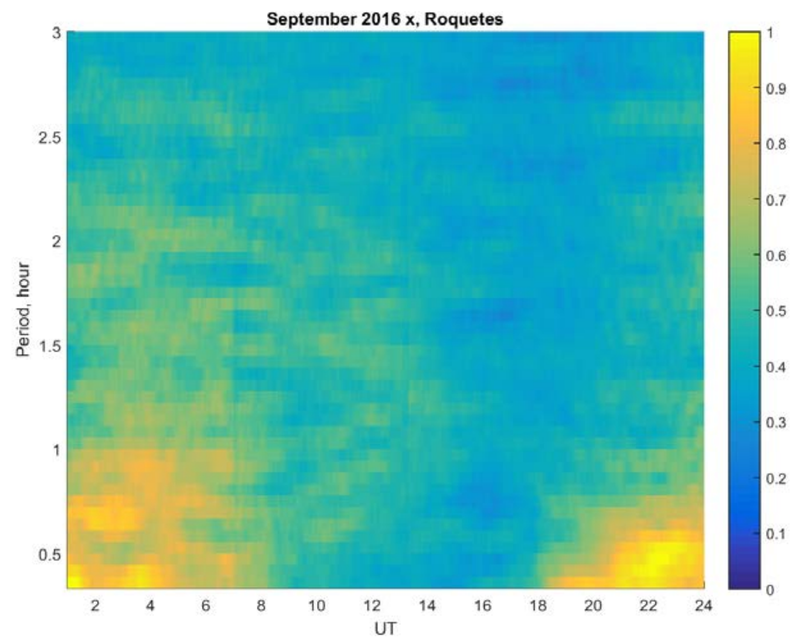
September 2016 x, Roquetes
Period, hour
UT
3
2.5
2
1.5
1
0.5
2 4 6 8 10 12 14 16 18 20 22 24
0 0.1 0.2 0.3 0.4 0.5 0.6 0.7 0.8 0.9 1

Comparison of North-South (x) and East-West (y) tilt components

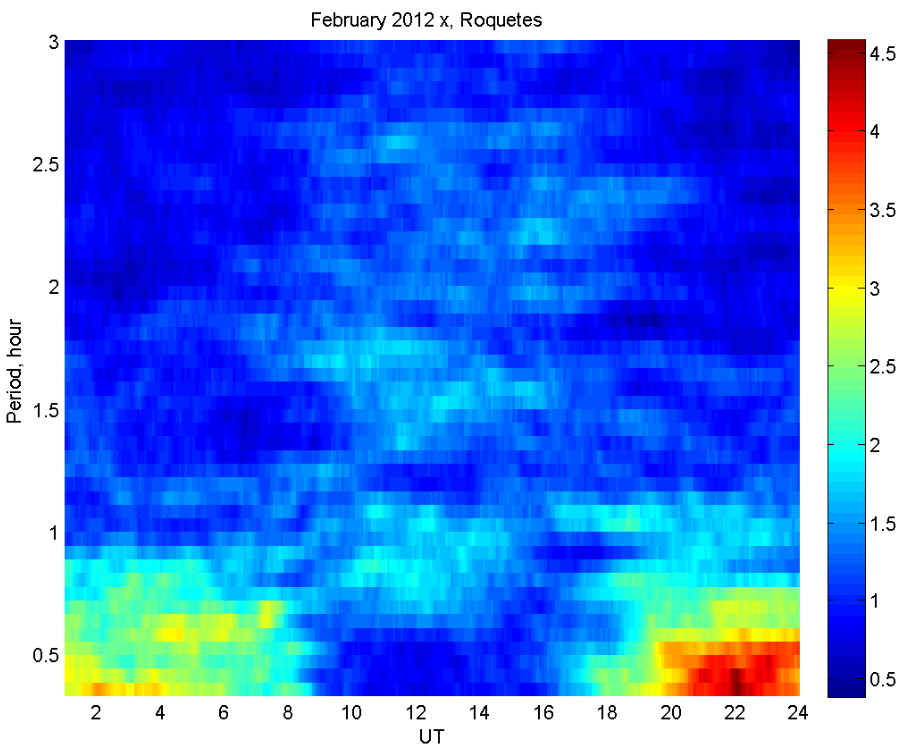

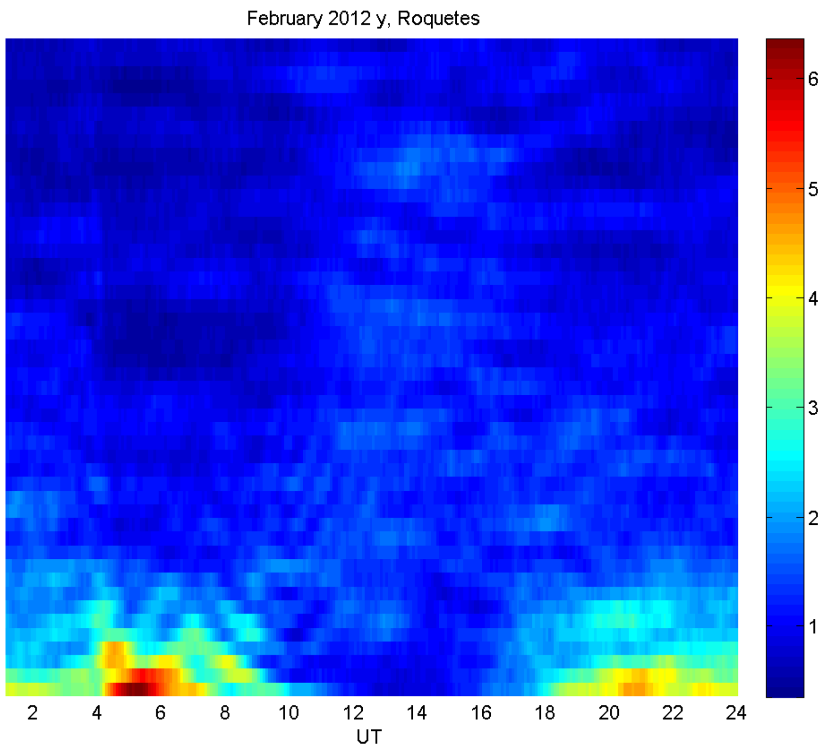

In February, the North-South tilt component demonstrates much stronger disturbances than East-West one, suggesting that in this month, TIDs propagated mostly southward.